How Far Does Risk Travel? The Social and Spatial Propagation of Systemic Risk

Huilin Zhang[a], Christos Giannikos[b]

[a]Department of Economics, City University of New York Graduate Center, 365 5th Ave, New York, USA

[b]Bert W. Wasserman Department of Economics and Finance, Zicklin School of Business, Baruch College, 55 Lexington Ave, New York, USA

Keywords: systemic risk, contagion, bank failure, social connectivity, sentiment, geographic proximity, social media

[1] This research did not receive any specific grant from funding agencies in the public, commercial, or not-for-profit sectors.

[2] Corresponding author Email addresses: hzhang1@gradcenter.cuny.edu (Huilin Zhang), Christos.Giannikos@baruch.cuny.edu (Christos Giannikos)

Abstract

This paper identifies how financial contagion spreads through physical and virtual spaces. Using an unbalanced panel of publicly traded U.S. bank holding companies from 2000 to 2023, we find that geographic proximity to failing institutions is positively associated with systemic risk across specifications. Social proximity exhibits no systematic association with systemic risk during normal times, as mixed signals wash out in aggregate. During acute stress episodes, however, social ties become a meaningful channel through which sentiment and panic propagate across the banking sector, consistent with Wake-up Call Theory and herding documented in the broader literature. These findings suggest that the channels through which systemic risk propagates extend beyond the balance sheet, and that monitoring the spatial and social architecture of banking networks may offer regulators early warning signals that traditional indicators miss.

On March 10, 2023, Silicon Valley Bank collapsed in just 36 hours. Two days later, Signature Bank failed in New York, and within seven weeks, First Republic Bank was seized. This rapid-fire sequence of failures raised a question traditional models were not built to answer: how does a bank run leap across the country between banks with no formal interbank exposures or common lenders? While the 2023 episode shares the underlying vulnerability of long-duration assets with the previous Global Financial Crisis in 2008, the transmission was fundamentally different. In 2023, banks did not collapse because they owed each other money — the vulnerabilities were on the balance sheet for anyone to see, but panic determined how fast and how far they spread. While Diamond and Dybvig (1983) focused on physical lines at the teller window, the 2023 episode demonstrated that the sequential service constraint now operates at the speed of wire transfers, and the informational cascades identified by Bikhchandani et al. (1992) are now mediated by real-time social media sentiment.

This paper investigates both social and geographic channels empirically. Using an unbalanced panel of publicly traded Bank Holding Companies from 2000 to 2023, we ask: does geographic proximity to bank failures elevate systemic risk exposure? Does social proximity, measured by Facebook's Social Connectedness Index (SCI), do the same? And does the sentiment traveling through social networks amplify or dampen these effects? Both channels are underexplored relative to the interbank linkage literature, and understanding them has direct implications for how regulators monitor and contain financial contagion.

The geographic channel operates through information and proximity. Banks with branches near a failing institution are more likely to share overlapping depositor bases, face scrutiny from the same local press, and be perceived by markets as exposed to similar risks. Despite a large literature on interbank contagion, the role of geographic proximity in systemic risk propagation remains largely unexplored empirically. This paper addresses that gap directly.

Social networks operate through a different but equally powerful channel, where information, sentiment, and panic transmit through communities of investors and depositors. Hong and Stein (1999) showed that information diffuses gradually across investors, generating momentum. Cookson et al. (2026) find evidence that Twitter activity accelerated SVB's collapse, with negative posts amplifying depositor withdrawals in real time. Both channels share a common thread: the propagation of information and fear through geographic and social networks that extend well beyond the interbank balance sheet.

While traditional systemic risk literature focuses on direct balance sheet linkages (Allen and Gale 2000, Freixas et al. 2000, Babus 2016), this paper contributes to an emerging body of work suggesting that information-based contagion can amplify financial contagion, particularly during episodes where coordinated depositor behavior drives stress. This phenomenon is not entirely modern; historical evidence from the 19th-century Irish banking panics shows that geographic and social ties were primary drivers of depositor behavior long before the digital age (Kelly and Ó Gráda, 2000). However, the 2023 banking crisis suggests a meaningful change in the velocity of these effects, as coordinated social media activity transformed localized sentiment into systemic panic with a speed faster than traditional monitoring frameworks could respond (Bales and Burghof, 2024). We do not claim social networks were the primary mechanism behind the large-value institutional wire outflows that initiated SVB's collapse, which were concentrated among VC and crypto-affiliated depositors with direct sectoral relationships. Rather, we examine how geographic and social networks serve as the informational infrastructure through which systemic risk propagates across the broader banking sector.

The third piece of our analysis concerns sentiment. A long tradition in behavioral finance documents that investor sentiment shapes risk-taking in ways inconsistent with rational expectations (De Long et al., 1990; Baker and Wurgler, 2006). Positive sentiment reduces perceived risk and lowers the cost of capital (Baker and Wurgler, 2006). But in highly connected networks, optimism can also coordinate correlated risk-taking and herding (Bikhchandani et al., 1992; Shiller, 2000). Adasi Manu and Qi (2023) find that banks led by socially connected CEOs carry higher systemic risk. The implication is that the same social connectivity that spreads good news efficiently can, when sentiment turns, amplify panic and coordinated risk-taking.

Systemic risk is measured using MES (Acharya et al., 2017) and ΔCoVaR (Adrian and Brunnermeier, 2016). While systemic risk lacks a single agreed-upon definition (Ellis et al., 2022), these two market-based measures are among the most widely adopted in the empirical banking literature (Laeven et al., 2016; Bostandzic and Weiss, 2018; Sedunov, 2016; Duan et al., 2021), and capture distinct but complementary dimensions of tail risk. MES captures a bank's own exposure during aggregate market downturns, while ΔCoVaR captures a bank's contribution to system-wide distress[1].

[1] Accounting-based measures such as non-performing loan ratios reflect credit outcomes with a lag and are subject to managerial discretion in classification, making them less suited to capturing the rapid propagation dynamics we study.

Our results show that geographic proximity to bank failures is positively associated with systemic risk across specifications, with the effect amplified during the GFC. A one standard deviation increase in geographic proximity is associated with a 0.03 standard deviation increase in MES in the pooled baseline, with an additional 0.05 standard deviation during the GFC. The social proximity findings tell a more nuanced story. Social connectedness to failing institutions does not systematically elevate systemic risk outside of acute stress periods. Outside of the 2023 crisis episode, idiosyncratic failures generate weak and diffuse signals through social networks that wash out in aggregate. During the 2023 banking stress episode, however, failures were large, high-profile, and rapidly amplified through digital channels. And it is precisely under these conditions that social proximity emerges as a meaningful risk channel.

We make three contributions. First, we provide evidence that both geographic and social proximity are quantitatively meaningful channels for systemic risk transmission, complementing the traditional focus on interbank linkages. Second, we show that sentiment's effect on systemic risk is not monotone but regime-dependent, with the social proximity channel activated specifically during acute stress episodes. Third, we contribute to the nascent literature connecting behavioral finance and macro-prudential risk, suggesting that monitoring the spatial and social architecture of banking networks may offer regulators early warning signals that balance sheet data alone cannot.

We caution that our results are associational. The absence of a clean quasi-experiment means we cannot make causal claims. But the consistency of our findings across outcomes, specifications, and subperiods raises a possibility that deserves serious attention: in an age of social media and geographically dispersed banking networks, the channels through which systemic risk propagates extend well beyond the interbank balance sheet.

1 Related Literature

This paper sits at the intersection of three strands of literature: systemic risk and financial networks, social networks in finance, and behavioral finance and sentiment.

Theoretical Motivation We ground our empirical analysis in three mechanisms that motivate why proximity shapes risk transmission. First, observational learning: depositors update beliefs about a bank's solvency by observing the actions of others (Bikhchandani et al. 1992, 1998), and geographic and social proximity define the set of actors they are most likely to observe. Second, the Wake-up Call Theory (Goldstein 1998; Ahnert and Bertsch 2022). SVB's collapse functioned as a public signal that prompted depositors at other institutions to suddenly scrutinize vulnerabilities they had previously ignored, including unrealized HTM losses and high uninsured deposit ratios. Proximity determined which depositor communities received and acted on this signal first. Third, sentiment: negative local sentiment in socially connected regions shapes how depositors collectively respond to stress signals, amplifying or dampening the effect of proximity on systemic risk (Cookson et al. 2026; Bales and Burghof 2024).

Geographic Proximity and Information Geography in banking is rooted in local economic conditions and relationship lending. Wheelock (1992) documents how historical bank failures reflected localized agricultural and economic collapses, where local credit shocks propagated through regionally concentrated lending relationships. While Calomiris and Mason (1994) find that geographic proximity did not drive contagion during the 1932 Chicago banking panic, where failures largely reflected weak fundamentals, our results suggest the geographic channel has become more relevant in an era of overlapping depositor bases and real-time information transmission. Outside the banking sector, Wu et al. (2022) show that reductions in physical distance lower external monitoring costs and improve information flow between firms and investors.

Financial Networks and Systemic Risk A foundational question in the systemic risk literature is whether dense interconnections among financial institutions amplify or dampen shocks. Allen and Gale (2000) and Freixas, Parigi, and Rochet (2000) show that more interconnected financial architectures can enhance resilience by distributing losses across the system. Blume (2011, 2013) models cascading failures through networks, while Krause and Giansante (2012) and Cabrales et al. (2017) analyze the trade-off between risk-sharing and contagion depending on the distribution of shocks and interbank lending structures. Acemoglu et al. (2015) reconcile these views, showing that moderate connectivity enhances stability while highly concentrated networks become fragile. Chan-Lau et al. (2009) show that network centrality, rather than market share alone, determines an institution's systemic footprint, giving rise to the "too-connected-to-fail" problem that balance sheet indicators miss. We complement this approach by examining channels that operate outside the balance sheet: geographic and social connectivity.

Social Networks and Behavioral Contagion A growing literature documents that social ties shape financial outcomes. Hong, Kubik, and Stein (2004) show that social interactions drive correlated investor participation in equity markets, while Flynn and Wang (2022) document analogous effects on bank deposit funding. Shiller (2000, 2017) argues that viral stories spreading through networks drives asset dynamics beyond fundamentals. Bailey et al. (2018) introduced the Social Connectedness Index (SCI), demonstrating that social ties predict economic behaviors ranging from trade flows to investment. Mizruchi and Stearns (2001) show that under uncertainty, bankers rely disproportionately on dense, high-trust networks for decision-making. The 2023 crisis highlighted the role of digital networks with coordinated social media activity and public attention accelerating bank failures in real time, as discussed earlier. Hirshleifer, Peng, and Wang (2025) show that firms in counties with high social centrality exhibit stronger and faster market reactions to public news, consistent with social connectedness facilitating rapid information incorporation — and, under stress, rapid panic transmission.

Sentiment and Liquidity as Buffers De Long et al. (1990) and Baker and Wurgler (2006) establish that investor sentiment shapes asset prices and risk-taking in ways inconsistent with rational expectations. Bikhchandani et al. (1992) formalize the theoretical conditions under which rational individuals herd based on the observed actions of others, and empirical work by Holmes et al. (2013) and Clements et al. (2017) further clarifies this behavior by distinguishing spurious from intentional herding, showing that correlated market behavior can arise from social observation rather than shared fundamentals. When sentiment turns negative, such herding and cascades can transform idiosyncratic shocks into systemic failures — a mechanism with direct banking-sector evidence in Fang et al. (2024), who find that negative media sentiment destabilizes deposits and elevates systemic risk. Liquidity provides a natural counterweight: Cornett et al. (2011) show that robust liquidity management buffers against deposit outflows during crises, motivating our hypothesis that liquid balance sheets attenuate the transmission of geographic contagion even when sentiment deteriorates.

2 Data and Methodology

2.1 Bank Data

We focus on all publicly traded bank holding companies in the United States, specifically the financial institutions that file a FR Y-9C report with the Federal Reserve each quarter. The FR Y-9C report collects basic financial data from a domestic bank holding company on a quarterly basis in the form of a balance sheet, an income statement, and detailed supporting schedules including off-balance-sheet items. Details on bank controls is in the Appendix section under Table A6 and Table A7. The sample is a quarterly unbalanced panel dataset from 2000-2023 and consists of 421 unique banks. The bank's daily equity returns are retrieved from CRSP, which are converted into quarterly returns. Financial Statement data is from CRSP/Compustat merged table on WRDS and Bank Regulatory Data from the Federal Reserve form FR Y-9C. For convenience, we refer to all of these financial institutions as banks.

2.2 Bank Failures

The definition of a bank failure according to the FDIC (Federal Deposit Insurance Corporation) is the closing of a bank by a federal or state banking regulatory agency [2]. A bank closure generally occurs when it is unable to meet its obligations to depositors and others. When a bank fails, the FDIC or a state regulatory agency takes control and either sells or dissolves the bank.

The bank failures in this paper are limited to FDIC-insured institutions, and the data [3] is obtained from the FDIC website and consist of a total of 569 commercial bank failures during the period 2000-2023. The approximated Assets in Millions at the time of failure is used as a weight in the proximity calculations later on. Then we match the banks onto the FR Y-9C call reports data based on name, city, and state to obtain the zipcode for the failed banks.

2.3 Social Connectedness Index

To measure the social proximity between a bank and failed bank locations, we use the Social Connectedness Index (SCI), introduced by Bailey et al. (2018) using Facebook data. The SCI measures the relative probability of a Facebook friendship link between a given Facebook user in location i and a user in location j. It is calculated by dividing the number of Facebook friends between locations i and j by the number of Facebook users in location i multiplied by the number of users in location j. The normalization in the denominator accounts for differences in population size or number of users across different areas. This allows the index to capture social connectivity patterns rather than just reflecting that larger areas naturally have more

[2] https://www.fdic.gov/bank-failures/when-bank-fails-facts-depositors-creditors-and-borrowers

[3] From the Federal Reserves Website links there are options to download csv files https://www.fdic.gov/resources/resolutions/bank-failures/failed-bank-list/ and https://www.fdic.gov/resources/resolutions/bank-failures/in-brief/index

connections [4].

$$Social\ Connectedness_{i,j} = \frac{Facebook\ Connections_{i,j}}{Facebook\ Users_i \times Facebook\ Users_j} \tag{1}$$

The SCI dataset provides values for geographic areas ranging from the zip code to the country level and represents an anonymized snapshot from a single point in time. In this paper, we utilize the county-level data with FIPS codes. The locations of Facebook users are assigned based on their information and activity on Facebook, including their public profile information as well as device and connection information. Since the data set is calculated based on Facebook friendships in March 2020, additional time points of the SCI could not be included in the model or in sensitivity analyses. In the next section, we will use the Social Connected Index (SCI) in the aggregate weighted social proximity measure between banks and bank failures.

2.4 Deposit-Weighted Exposure to Bank Failures

We construct bank-quarter measures of exposure to bank failures by combining each bank's geographic deposit footprint with the proximity of that footprint to counties experiencing failures in the same quarter. For each bank b in quarter t, the exposure measure captures how concentrated a bank's deposit base is in counties that are either geographically close to or socially connected with counties experiencing bank failures, weighted by the size of those failures.

We focus on FDIC-recorded bank failures because they represent discrete and observable events that generate the informational signals our proximity measures are designed to capture. Distress indicators lack these properties: there is no agreed-upon definition of bank distress, non-performing loan classifications are subject to managerial discretion in provisioning decisions, and regulatory forbearance can delay or suppress observable failure signals [5]. As a result, distress is a noisy measure for this setting, as a bank can be distressed for months or years without a clean event date, making it impossible to pin down when the informational signal entered the network.

A failure recorded by the FDIC has a definitive date and an immediate market impact. This

[4] More details on methodology and scaling of the Social Connectivity Index available here: https://dataforgood.facebook.com/dfg/docs/methodology-social-connectedness-index

[5] Regulatory forbearance refers to instances where supervisors permit undercapitalized institutions to continue operating rather than triggering formal closure, so distress-based measures can conflate vulnerability with supervisory tolerance. Loveland (2016) documents systematic underreporting of loan impairment prior to closure during the GFC, illustrating how accounting-based distress indicators may generate muted or delayed signals relative to the actual risk present in the network.

approach follows recent work on the 2023 episode that similarly treats actual failures as the identifiable shock through which network transmission operates (Cookson et al., 2026; Bales and Burghof, 2024; Choi et al., 2023). A related concern is that large institutions that are distressed but receive implicit guarantees or bailouts never appear in the FDIC failure sample. At the same time, these institutions did not generate the same sharp informational shock that a discrete closure produces. Whether their distress propagated through similar geographic and social channels remains an open question that requires a different empirical design.

The exposure measure combines three components: deposit-share weights across a bank's branch network, failure-size weights for each failed county, and a proximity kernel. We define each in turn.

2.4.1 Bank Footprint Weights (Summary of Deposits)

Let i index U.S. counties. Using the FDIC Summary of Deposits (SOD), we compute each bank's county deposit shares. For bank b in year y, define the deposit-share weight in county i as:

$$w_{b,i,y} \;=\; \frac{\text{Deposits}_{b,i,y}}{\sum_{i'} \text{Deposits}_{b,i',y}}, \tag{2}$$

where $\text{Deposits}_{b,i,y}$ is bank b's total deposits in county i in year y. These weights satisfy $\sum_i w_{b,i,y} = 1$ over counties where the bank operates in that year. We map annual SOD weights to quarters by setting $w_{b,i,t} \equiv w_{b,i,y(t)}$, where $y(t)$ denotes the calendar year containing quarter t.

2.4.2 Failure Shocks (FDIC Bank Failures)

Let j index counties that experience bank failures. For each quarter t, define $\mathcal{F}_t$ as the set of counties with at least one bank failure during quarter t. We optionally weight each failed county by the size of failures occurring there. Let $\text{Assets}_{j,t}$ denote the total assets of failed institutions in county j during quarter t (aggregated if multiple failures occur in the same county-quarter). The county-level failure size weight is:

$$s_{j,t} \;=\; \log\big(\text{Assets}_{j,t}\big). \tag{3}$$

2.4.3 Geographic Proximity: Nearby Failure Exposure

We convert physical distance between counties into a "closeness" kernel. Let d_{ij} denote the great-circle distance (in kilometers) between county centroids of counties i and j. We define the geographic kernel as:

$$k_{ij}^{\text{geo}} \;=\; \frac{1}{\max(d_{ij},\,1)}, \tag{4}$$

where we cap the minimum distance at 1 km to avoid infinite values when $i = j$ (same-county exposure). The bank–quarter geographic exposure to failures is then:

$$\text{Geographic Proximity}_{b,t} \;=\; \sum_{i \in \mathcal{C}_b} w_{b,i,t} \left(\sum_{j \in \mathcal{F}_t} s_{j,t}\, k_{ij}^{\text{geo}} \right), \tag{5}$$

where $\mathcal{C}_b$ is the set of counties in which bank b has deposits (in year $y(t)$). Intuitively, $\text{GEO}_{b,t}$ is a deposit-share-weighted average of how geographically close the bank's footprint is to failed counties in quarter t, with larger failures receiving greater weight through $s_{j,t}$.

We use this continuous inverse-distance kernel measure because each bank holds deposits across counties at varying distances from any given failure. The continuous kernel allows exposure to vary smoothly with distance across a bank's full deposit footprint. We verify in robustness checks that the geographic channel persists when headquarter region × year-quarter fixed effects absorb any spatial clustering in unobservables (Tables A4 and A3).

2.4.4 Social Proximity (SCI): Socially Connected Failure Exposure

The social exposure measure is constructed similarly to the geographic measure in equation 5, replacing the geographic kernel k_{ij}^{geo} with Facebook's Social Connectedness Index (SCI) SCI_{ij} introduced in 2.3.

The bank–quarter social exposure to failures is:

$$\text{Social Proximity}_{b,t} \;=\; \sum_{i \in \mathcal{C}_b} w_{b,i,t} \left(\sum_{j \in \mathcal{F}_t} s_{j,t}\, \text{SCI}_{ij} \right). \tag{6}$$

This measure replaces geographic closeness with social connectedness: exposure is higher when a bank's deposit footprint is concentrated in counties that are more socially connected to counties experiencing failures in the same quarter, again scaled by failure size $s_{j,t}$.

Both exposure measures are constructed at the bank–quarter level by combining (i) annual county deposit shares from SOD, (ii) the set of failure counties each quarter, and (iii) either geographic closeness k_{ij}^{geo} or social connectedness SCI_{ij}. One asymmetry across measures is worth noting: the geographic kernel includes same-county exposure (capped at 1 km), while the

SCI-based measure excludes self-connections, as Facebook's SCI data does not report within-county social connectedness values.

2.5 Social Media Sentiment Measure

In this paper, we explore social media sentiment, proxied by Twitter Sentiment Geographical Index provided by Chai (2023) [6], as a channel of propagation of systemic risk through social ties. Twitter, now rebranded as X, is a free social networking site where users broadcast short posts known as tweets, which can contain text, videos, photos, or links. The index of this sentiment measure is developed by training a BERT-based multi-lingual sentiment classification model based on a labelled database and applies it to a global geotagged Twitter archive (containing 10 billion posts) from the Center of Geographic Analysis (CGA) of Harvard. The BERT model learns to represent text as a sequence of vectors using self-supervised learning. The computation of the index begins with imputing a sentiment score, which is the probability of a post being classified as a post with a positive mood, for every post and then aggregating them to multiple administrative levels (i.e., city/county, state, and country) daily.

The Twitter Sentiment Geographical Index (TSGI) dataset measures X/Twitter sentiment on a continuous scale ranging from 0 (most negative) to 1 (most positive). The raw dataset is available at a daily frequency, and for this analysis, we averaged the daily sentiment scores at the county level within each quarter to construct a quarterly sentiment index.

2.6 Sample Windows for Geographic vs Social Exposure

We construct geographic exposure measures over the full 2000–2023 sample, using all available bank failure and bank holding company data. Our analysis of social connectedness exposure focuses on 2013–2023, for two reasons. First, the sentiment measure used in interaction analyses is not available prior to 2012. Second, applying a time-invariant social connectedness matrix over multiple decades would require an implausibly strong stability assumption. Restricting to a one-decade window mitigates this concern while still capturing persistent cross-sectional patterns in social connectedness.

This restriction is further supported by evidence that county-level social connectivity is remarkably stable over time, rooted in durable features of the economic landscape such as historical

[6] See Twitter Sentiment Geographical Index (https://doi.org/10.7910/DVN/3IL00Q)

migration patterns, family ties, and physical infrastructure (Bailey et al 2018, 2020). The underlying probability of connection between geographic locations reflects these stable social structures rather than platform-specific user behavior. Throughout, the SCI is treated as a fixed cross-sectional matrix capturing persistent social ties across counties within the 2013–2023 period, over which Facebook's user base is both mature and relatively stable.

2.7 Systemic Risk Measures

We use two market-based measures of systemic risk as our primary dependent variables: Marginal Expected Shortfall (MES) developed by Acharya et al. (2017) and ΔCoVaR developed by Adrian and Brunnermeier (2016). Unlike simple return correlations, which capture average comovement across the full return distribution, these measures are specifically designed to quantify tail dependencies and asymmetric risk spillovers during periods of distress, making them better suited to studying contagion. Their use in fixed effects panel settings to identify cross-sectional drivers of systemic risk is well established in the empirical banking literature (Laeven et al., 2016; Bostandzic and Weiss, 2018; Sedunov, 2016; Duan et al., 2021).

While this approach limits the sample to publicly traded bank holding companies, these entities are on average larger and more systemically important, and their distress poses a greater threat to financial stability. The two measures are calculated in Matlab using the Systemic Risk package developed by Belluzzo (2024). Throughout the systemic risk definitions and regression specifications that follow, subscript b indexes banks and t indexes quarters. MES focuses on a firm's exposure to aggregate tail shocks, quantifying its expected capital loss during a systemic crisis. ΔCoVaR measures a firm's contribution to the overall financial system's distress, calculated as the change in the financial system's VaR when institution b is in distress versus at its normal (median) state.

2.7.1 Definition of systemic risk using ΔCoVaR

ΔCoVaR measures which financial institution contributes most to a systemic crisis and is defined as the difference between the VaR of the financial system conditional on firm b being in distress and the VaR of the system conditional on firm b being in its median state.

$$\Pr\left(r_{m,t} \leq \mathrm{CoVaR}_{b,t}^{m|\mathrm{C}(r_b,t)} \;\middle|\; \mathrm{C}(r_b,t)\right) = \alpha \tag{7}$$

where $r_{m,t}$ is market return, $\mathrm{C}(r_b, t)$ is the event when the individual firm stock return is at its bottom α probability level.

$$\Delta\mathrm{CoVaR}_b(\alpha) \;=\; \mathrm{CoVaR}_{b,t}^{m|r_b(t)=\mathrm{VaR}_{b,t}(\alpha)} \;-\; \mathrm{CoVaR}_{b,t}^{m|r_b(t)=\mathrm{median(r_{b,t})}}. \tag{8}$$

Following Adrian and Brunnermeier (2016), we set $\alpha = 0.05$ and control for state variables: VIX index of stock market volatility, the change in the three-month Treasury bill rate, the liquidity spread between the three-month repo rate and the three-month T-bill rate, the change in the slope of the yield curve, and the change in the credit spread between BAA-rated bonds and the Treasury rate. The term $\mathrm{CoVaR}_{b,t}^{m|r_b(t)=\mathrm{VaR}_{b,t}(\alpha)}$ is the Value-at-Risk of the market conditional on firm b being in distress, while $\mathrm{CoVaR}_{b,t}^{m|r_b(t)=\mathrm{VaR}_{b,t}(\alpha)} - \mathrm{CoVaR}_{b,t}^{m|r_b(t)=\mathrm{median(r_{b,t})}}$ is the market VaR conditional on firm b being in its median state. ΔCoVaR is estimated using quantile regressions.

2.7.2 Definition of systemic risk using MES

Acharya et al. (2017) propose marginal expected shortfall (MES) as a measure of systemic risk. MES estimates bank b's losses when the entire market is doing poorly. In other words, how the risk taking of the financial market adds to bank b's overall risk. MES is measured at the bank level at the $\alpha = 5\%$ risk level using daily equity returns from CRSP.

Value-at-Risk (VaR) at level α is the most the bank loses with confidence $1 - \alpha$:

$$\Pr(R < -VaR_\alpha) \;=\; \alpha. \tag{9}$$

The Expected Shortfall, expected loss conditional on the loss being greater than the VaR, at level α is then given by

$$\mathrm{ES}_\alpha = -\sum_b y_b\, E\left[r_b \,\middle|\, R \leq -\mathrm{VaR}_\alpha\right]$$

where r_b is the return of bank b, y_b is the market capitalization of bank b, and R is the market return. The partial derivative of ES with respect to y_b is referred to as the Marginal Expected Shortfall (MES) of bank b.

$$\mathrm{MES}_b \;=\; \frac{\partial \mathrm{ES}_\alpha}{\partial y_b} \;=\; -\,E\big[R_b \,\big|\, R \leq -\,\mathrm{VaR}_\alpha(R)\big] \tag{10}$$

measures the expected loss in bank b's equity return, given that the aggregate market portfolio R is in the tail (i.e., below $-\mathrm{VaR}_\alpha$).

2.8 Empirical Framework

Our empirical design examines two channels. For geographic proximity, we expect that greater exposure to nearby failure counties elevates systemic risk, with the effect attenuated in banks holding more liquid balance sheets. For social proximity, we expect no systematic effect in normal times — social networks transmit mixed signals in the absence of a common shock — but a meaningful risk channel during the 2023 episode, conditioned on the local sentiment environment.

2.9 Model Specifications

We estimate MES and ΔCoVaR separately as dependent variables in the following baseline model:

$$\mathrm{SR}_{bt} = \mu_b + \lambda_t + \beta_1 \,\mathrm{Proximity}_{b,t-1} + \gamma' \mathbf{X}_{b,t-1} + \epsilon_{bt}.$$

where SR_{bt} denotes the systemic risk of bank b in period t. $\mathrm{Proximity}_{b,t-1}$ is the main explanatory variable capturing a bank's geographic or social proximity to bank failures in the previous period, with effect measured by β_1. $\mathbf{X}_{b,t-1}$ is a vector of lagged bank-level controls including log assets, unrealized HTM losses, cash, liquid assets, loans, leverage, deposit funding, and non-interest income, following Laeven et al. (2016), Brunnermeier et al. (2020), and Choi et al. (2023). μ_b denotes bank fixed effects and λ_t denotes year-quarter fixed effects, absorbing time-invariant bank heterogeneity and common macroeconomic shocks respectively. Standard errors are clustered at the bank level.

The specific vulnerability that SVB's failure made salient — unrealized HTM losses concentrated in institutions with high uninsured deposit ratios — was in principle publicly observable through regulatory filings. In practice, geographic and social proximity likely determined which depositor communities were positioned to rapidly interpret and act on these disclosures. Our bank-level controls for unrealized HTM losses and deposit funding ratios absorb within-bank vulnerability differences. The proximity coefficients therefore capture network-level variation in how the signal propagated, over and above individual balance sheet exposure. To reduce reverse causality concerns, all explanatory variables are lagged one period, ensuring they are predetermined relative to the outcome.

We extend this baseline in two directions. First, we interact geographic proximity with bank-level liquidity to test whether liquid balance sheets buffer exposure to nearby failures. Second, we interact social proximity with local Twitter sentiment to examine whether the information environment amplifies or dampens the association between social proximity and systemic risk. These heterogeneity analyses are discussed in Section 4.

3 Descriptive Statistics

Table 1 displays the summary statistics for our two samples of publicly traded Bank Holding Companies (BHCs). Because variable scales differ substantially across measures, all variables are standardized prior to estimation. Panel A covers 2000–2023 (N = 28,069 bank-quarter observations) and is used for the geographic proximity analysis. Panel B covers 2013–2023 (N = 10,738 observations) and is used for the social proximity analysis, which uses the Facebook Social Connectedness Index (SCI) to measure inter-county social network ties. SCI captures stable, long-term social structures that are unlikely to shift substantially over a decade, but applying a fixed network to two full decades of data would be too strong an assumption for the full 2000-2023 sample. Therefore we limit the sample to 2013 onward for the social proximity analysis. The 2013-2023 sample in Panel B also includes Average Twitter Sentiment as an additional control to examine whether public sentiment heightens or dampens systemic risk alongside social network effects.

Table 1: Summary Statistics (Public BHCs)

Panel A: 2000–2023

Variable	N	Mean	SD	Min	Max
Geographic Proximity	28069	0.14	0.84	0.00	33.04
Social Proximity	28069	203722.12	985598.48	0.00	59027748.71
MES	28069	0.02	0.02	0.00	0.20
$\Delta CoVaR$	28069	0.01	0.00	0.00	0.06
Log Assets	28069	15.03	1.79	11.93	22.13
Leverage	28069	10.20	25.02	0.23	3713.42
Unrealized HTM Losses Book Ratio	28069	-0.00	0.04	-0.93	1.00
Liquid Asset Ratio	28069	0.23	0.11	0.00	0.81
Cash Asset Ratio	28069	0.05	0.05	0.00	0.46
Loans Asset Ratio	28069	0.63	0.19	0.00	0.96
Deposits Liabilities Ratio	28069	0.84	0.14	0.00	1.00
Non-Interest Income Ratio	28069	0.20	0.14	-2.29	0.99

Panel B: 2013–2023

Variable	N	Mean	SD	Min	Max
Geographic Proximity	10738	0.06	0.37	0.00	13.72
Social Proximity	10738	88929.71	463927.66	0.00	23293107.44
MES	10738	0.02	0.01	0.00	0.13
$\Delta CoVaR$	10738	0.01	0.00	0.00	0.04
Log Assets	10738	15.71	1.80	12.62	22.10
Leverage	10738	8.91	5.06	0.37	241.36
Unrealized HTM Losses Book Ratio	10738	-0.00	0.05	-0.60	0.71
Liquid Asset Ratio	10738	0.23	0.11	0.01	0.91
Cash Asset Ratio	10738	0.06	0.05	0.00	0.46
Loans Asset Ratio	10738	0.66	0.14	0.00	0.96
Deposits Liabilities Ratio	10738	0.87	0.13	0.00	1.00
Non-Interest Income Ratio	10738	0.23	0.15	-2.29	0.99
Average Twitter Sentiment	10738	0.60	0.07	0.21	0.84

Figure 1 illustrates the dynamics of systemic risk and bank failures across time, and highlights three stress episodes: the Global Financial Crisis (GFC, 2007–2009), the COVID-19 pandemic (2020–2021), and the 2023 banking turmoil. Panel (a) shows that bank failure counts peaked sharply during the GFC, with over 50 failures in a single year, before gradually declining through the mid-2010s and reaching near zero thereafter.

While bank failure counts in 2023 were low, Figure 1 Panel (b) highlights that a small number of high-profile institutions (Silicon Valley Bank, Signature Bank, and First Republic) experienced severe bank runs and were subsequently seized by regulators, with their combined assets at closing exceeding \$500 billion. Panel (c) confirms that MES and ΔCoVaR, the two most widely used systemic risk measures in the literature, co-move closely throughout the sample period and spike during the crisis episodes.

We use the GFC and 2023 stress episodes for our heterogeneity analysis in Section 4, as these banking crises involved specific collapses that triggered panic and bank runs in other institutions, leading to system-wide risk. While systemic distress was most acute during the GFC, the 2023 banking turmoil exhibited a comparable pattern of system-wide disruption. Focusing on these two episodes allows us to examine whether risk propagation through geographic and social networks intensifies when contagion and bank runs are the primary drivers of systemic stress.

Figure 1: Systemic risk and bank-failure time series.

(a) Bank failures (count)

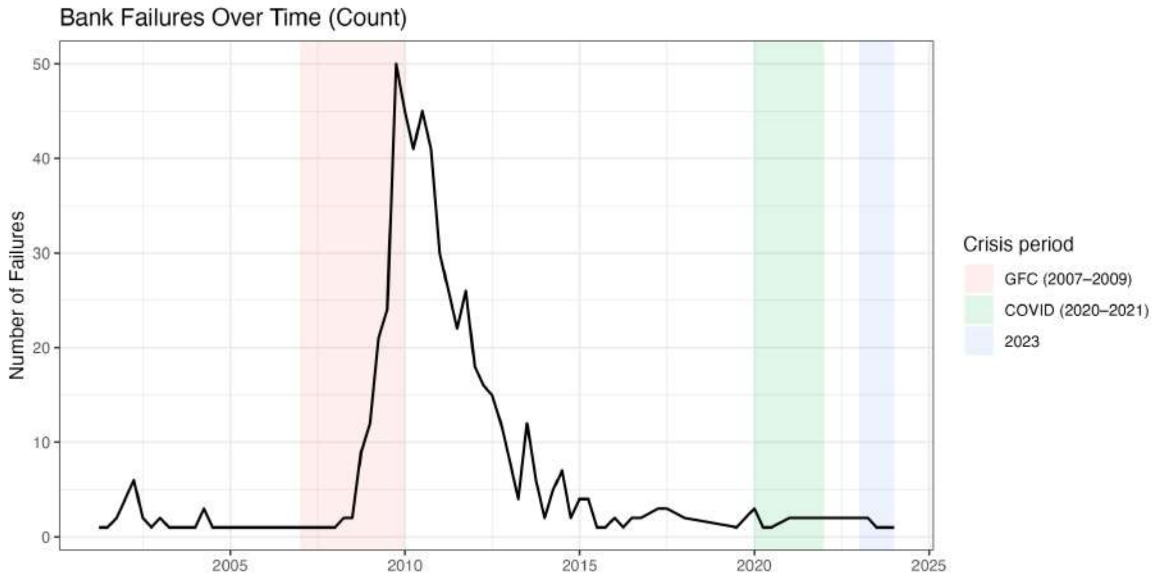

(b) Bank failures (assets)

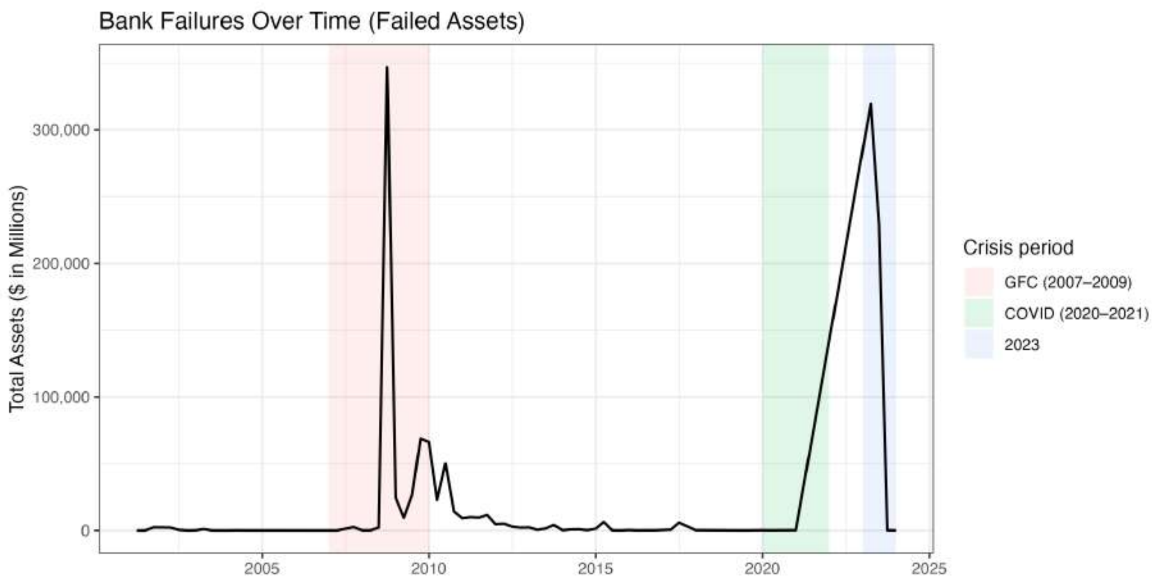

(c) Average MES and Δ CoVaR (z-score)

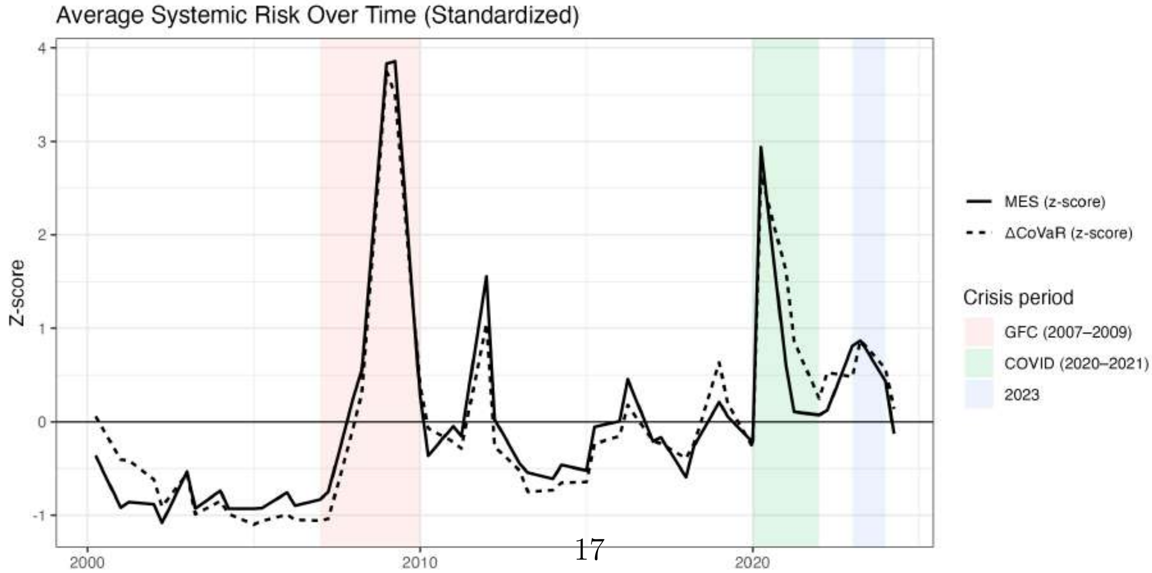

Figures 2 and 3 show the spatial distribution of BHC headquarters and average assets by county, providing context for the geographic footprint of the banking sector across the 2000-2023 sample period. Bank presence is concentrated in major financial centers along the coasts and in the Northeast, with sparser coverage in the Midwest. While the coastal regions and major urban centers host more BHC headquarters, the size of those institutions is fairly evenly distributed across counties.

Figures 4 and 5 map total and average assets of failed banks by county, aggregated across all FDIC-reported failures from 2000–2023. While failures occurred nationwide, most are concentrated in California, and parts of the Midwest and South.

Figure 2: Heatmap Number of BHCs by county

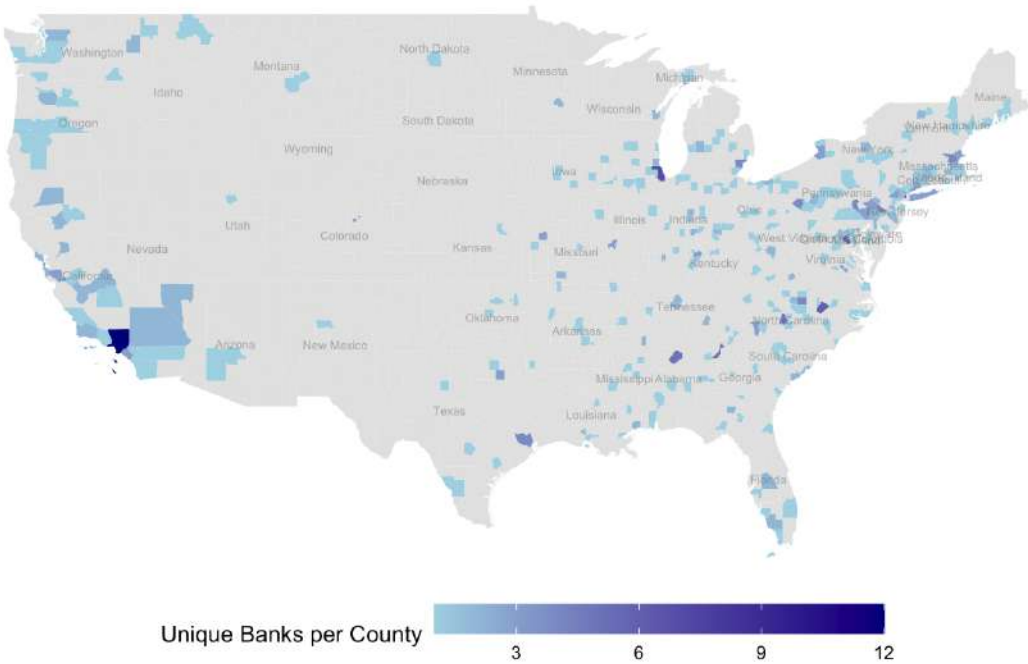

Figure 3: Heatmap - Average BHC Assets by County

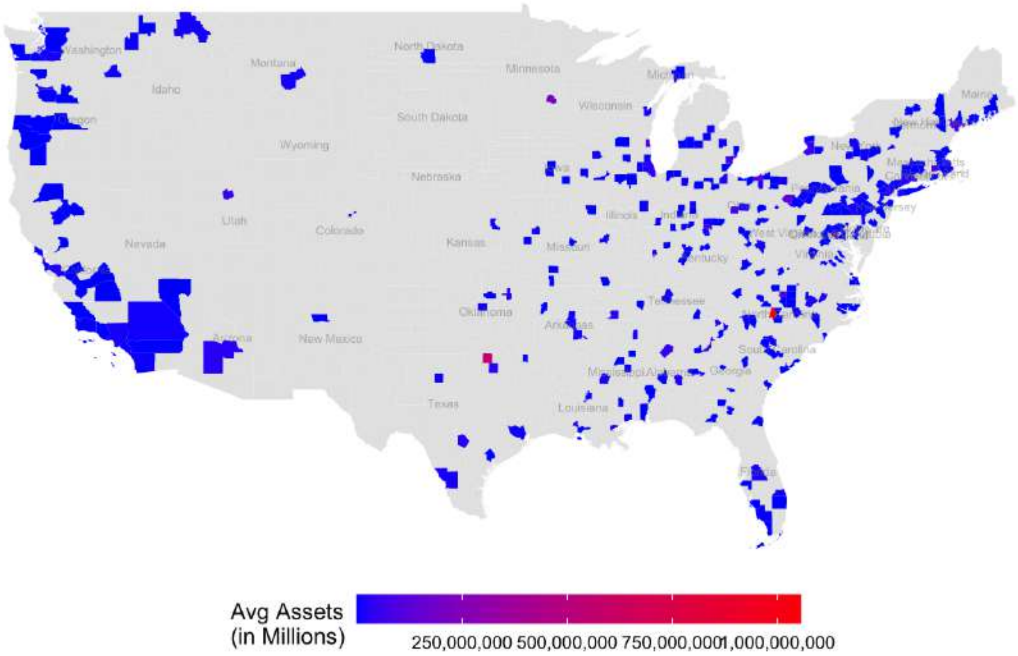

Figure 4: Heatmap Total Assets of Failed Banks by County

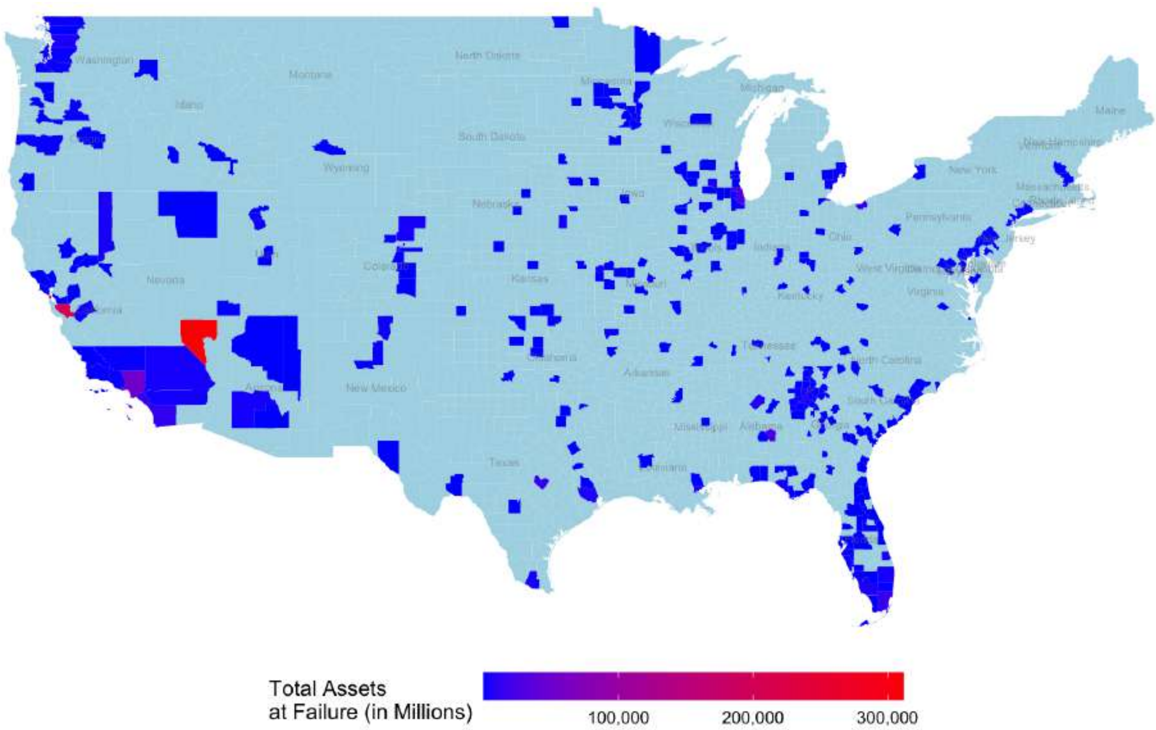

Figure 5: Heatmap Average Assets of Failed Banks by County

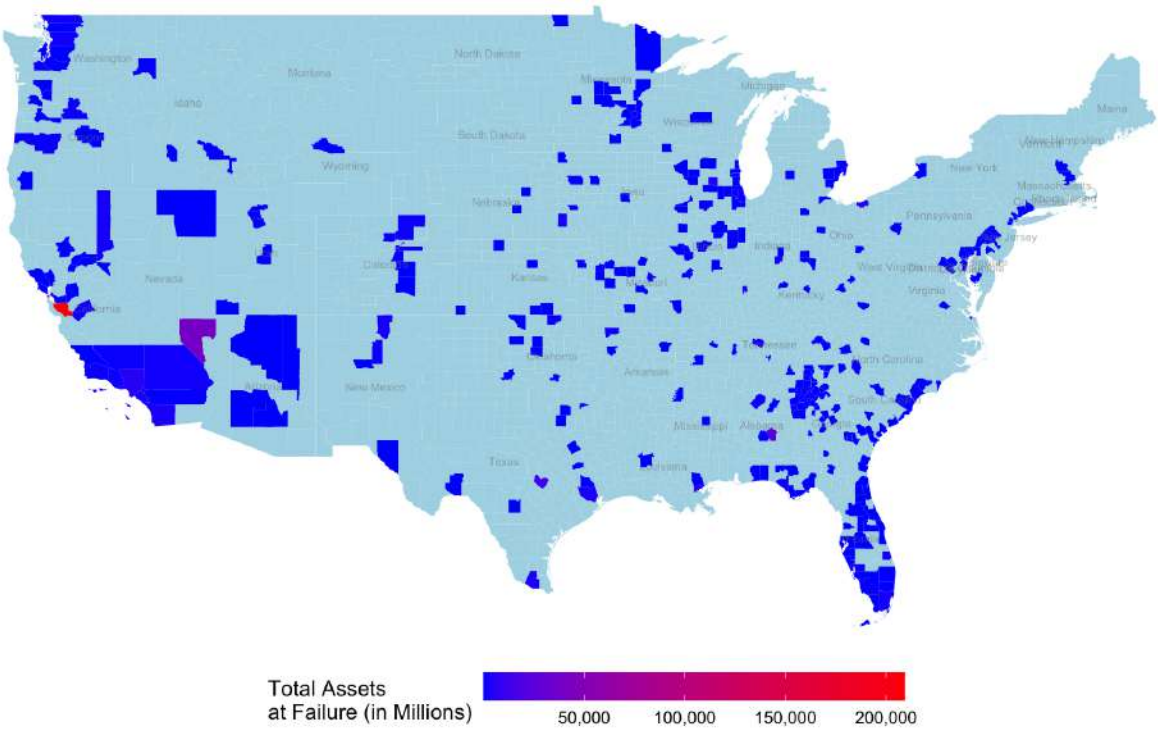

4 Results

4.1 Systemic Risk and Proximity to Bank Failures

Table 2 reports the baseline results. Panel A shows that geographic proximity to bank failures is positively and significantly associated with systemic risk across both measures. A one standard deviation increase in geographic proximity is associated with a 0.03 standard deviation increase in MES and a 0.02 standard deviation increase in ΔCoVaR, both significant at the 1% and 5% levels respectively. Panel B shows that social proximity alone does not significantly elevate systemic risk in either specification. This is not surprising: social networks transmit both stabilizing and destabilizing information, and their net effect in normal times is ambiguous. The social channel becomes meaningful when conditioned on the information environment, as shown in Sections 4.3 and 4.4.

Bank control variables are included in all specifications but omitted from the main tables for brevity. Full estimates are reported in Appendix Tables A1 and A2. Control coefficients follow expected patterns: larger banks and higher loan shares are associated with greater systemic risk, while more liquid balance sheets, deposit funding, and non-interest income are associated with lower systemic risk, consistent with Laeven et al. (2016), Brunnermeier et al. (2020), and Choi et al. (2023).

Because the Social Connectedness Index is available from a single point in time and the sentiment data begins in 2012, the social proximity analysis is restricted to 2013–2023; estimating geographic and social proximity jointly over a common window is therefore left to future work as richer time-varying social network data become available.

4.2 Moderating Channels: Liquidity and Sentiment

We extend the baseline specification to examine two moderating channels, each motivated by the mechanism through which the respective proximity measure operates. For geographic proximity, the natural moderator is bank-level liquidity. Banks with more liquid balance sheets can absorb deposit outflows from nearby failures without resorting to fire sales, reducing local stress transmission. For social proximity, the natural moderator is sentiment: social networks transmit information, and whether that information amplifies or reduces risk depends on whether the prevailing signal is one of fear or reassurance.

Table 2: Baseline Results

Panel A: Geographic Proximity (2000–2023)

Dependent Variables:	MES	$\Delta CoVaR$
Model:	(1)	(2)
Variables		
Geographic Proximity (t-1)	0.03***	0.02**
	(0.008)	(0.007)
Bank FE	Yes	Yes
Time FE	Yes	Yes
Bank Controls	Yes	Yes
Fit statistics		
Observations	27,598	27,598
R^2	0.66175	0.70845

Panel B: Social Proximity (2013–2023)

Dependent Variables:	MES	$\Delta CoVaR$
Model:	(1)	(2)
Variables		
Social Proximity (t-1)	-0.003	0.007
	(0.004)	(0.004)
Bank FE	Yes	Yes
Time FE	Yes	Yes
Bank Controls	Yes	Yes
Fit statistics		
Observations	10,374	10,374
R^2	0.79290	0.83737

Notes: Bank controls are included in all regressions but not reported.

$$
\begin{aligned}
\mathrm{SR}_{b,t} = \mu_b + \lambda_t + \beta_1 \,\mathrm{Proximity}_{b,t-1} + \beta_2 \,\mathrm{Moderator}_{b,t-1} \\
+ \beta_3 \,(\mathrm{Proximity} \times \mathrm{Moderator})_{b,t-1} + \gamma' \,\mathbf{X}_{b,t-1} + \epsilon_{b,t}
\end{aligned}
$$

where $\mathrm{Moderator}_{b,t-1}$ is the liquid asset ratio in Panel A and average Twitter sentiment in Panel B. The coefficient of interest is β_3.

Table 3 reports the results. In Panel A, the interaction between geographic proximity and liquidity is negative and significant for MES (-0.01^*). Notably, the liquid asset ratio alone does not reduce systemic risk, but it significantly attenuates the transmission of stress from nearby failures, suggesting that liquidity operates specifically as a buffer against local contagion rather than as a general risk mitigant.

The divergent results between MES and ΔCoVaR are noteworthy. Löffler and Raupach (2018) show that MES and ΔCoVaR capture fundamentally different dimensions of risk: the former reflects a bank's vulnerability to aggregate tail events, while the latter captures its contribution to system-wide distress. The significant coefficient for MES but not ΔCoVaR indicates that liquidity protects the individual bank from contagion exposure, but does not reduce its contribution to system-wide distress. This has a direct regulatory interpretation. Liquidity is an internal shield: it protects the individual bank from absorbing deposit outflows when the system is under distress, reducing its own tail risk exposure as measured by MES. But liquidity does not dissolve the systemic externality. A bank's contribution to system-wide distress, captured by ΔCoVaR, is governed by structural interconnectedness that liquidity alone cannot offset. Requiring banks to hold more liquid assets is therefore a micro-prudential tool that reduces own-firm vulnerability without necessarily reducing systemic footprint.

In Panel B, neither social proximity nor its interaction with sentiment reaches statistical significance. This is consistent with social networks acting as a noisy channel during the full 2013–2023 period, transmitting conflicting signals that wash out in aggregate. As we show in Section 4.3, the risk-amplifying role of social proximity is highly regime-dependent, emerging only when conditioned on a crisis state.

Table 3: Heterogeneity: Liquidity and Sentiment

Panel A: GEO × Liquidity (2000–2023)

Dependent Variables:	MES	$\Delta CoVaR$
Model:	(1)	(2)
Variables		
Geographic Proximity (t-1)	0.03***	0.02**
	(0.008)	(0.008)
Liquid Asset Ratio (t-1)	-0.007	0.01
	(0.02)	(0.02)
Geographic Proximity (t-1) × Liquid Asset Ratio (t-1)	-0.01*	-0.008
	(0.007)	(0.007)
Bank FE	Yes	Yes
Time FE	Yes	Yes
Bank Controls	Yes	Yes
Fit statistics		
Observations	27,598	27,598
R^2	0.66193	0.70851

Panel B: SCI × Sentiment (2013–2023)

Dependent Variables:	MES	$\Delta CoVaR$
Model:	(1)	(2)
Variables		
Social Proximity (t-1)	-0.005	0.004
	(0.005)	(0.005)
Average Twitter Sentiment (t-1)	-0.03	-0.04**
	(0.02)	(0.02)
Social Proximity (t-1) × Average Twitter Sentiment (t-1)	-0.004	-0.006
	(0.005)	(0.005)
Bank FE	Yes	Yes
Time FE	Yes	Yes
Bank Controls	Yes	Yes
Fit statistics		
Observations	10,374	10,374
R^2	0.79300	0.83764

Notes: Bank controls are included in all regressions but not reported.

4.3 Proximity to Bank Failures during Crisis

We next examine whether the effects of geographic and social proximity are amplified during crisis periods. We interact each proximity measure with crisis window indicators for the Global Financial Crisis (GFC) and the 2023 banking stress episode:

$$\begin{aligned}\mathrm{SR}_{b,t} = \mu_b + \lambda_t + \beta_1\,\mathrm{Proximity}_{b,t-1} + \beta_2\,\mathbf{1}_{\mathrm{GFC}} + \beta_3\,(\mathrm{Proximity} \times \mathbf{1}_{\mathrm{GFC}})_{b,t-1} \\ + \beta_4\,\mathbf{1}_{2023} + \beta_5\,(\mathrm{Proximity} \times \mathbf{1}_{2023})_{b,t-1} + \gamma'\,\mathbf{X}_{b,t-1} + \epsilon_{b,t}\end{aligned}$$

where $\mathbf{1}_{\mathrm{GFC}}$ and $\mathbf{1}_{2023}$ are indicators for the Global Financial Crisis and 2023 banking stress episode respectively. The coefficients of interest are β_3 and β_5, which capture whether proximity effects are significantly stronger during each crisis period relative to normal times.

Crisis window indicators are defined as:

$$\mathbf{1}_{\mathrm{GFC},t} = \begin{cases} 1 & \text{if } t \in [2008\text{ Q1, } 2009\text{ Q4}] \\ 0 & \text{otherwise} \end{cases}$$

$$\mathbf{1}_{2023,t} = \begin{cases} 1 & \text{if } t \in [2023\text{ Q1, } 2023\text{ Q4}] \\ 0 & \text{otherwise} \end{cases}$$

The GFC window spans the onset of the financial crisis through the trough of the recession. The 2023 window covers the calendar year of the SVB, Signature Bank, and First Republic failures.

Table 4 reports the results. In Panel A, geographic proximity is significantly amplified during the GFC for both MES (0.05^{***}) and ΔCoVaR (0.04^{**}), consistent with physical proximity becoming a more potent contagion channel when system-wide stress is elevated. The interaction with the 2023 crisis window is negative and insignificant, suggesting that the geographic channel did not intensify further during 2023 relative to normal times.

In Panel B, social proximity alone remains insignificant, but its interaction with the 2023 crisis window is positive and significant for ΔCoVaR (0.39^{*}). This indicates that during the 2023 episode, socially connected banks contributed more to system-wide distress, consistent with social networks serving as a conduit for coordinated panic when stress is concentrated and rapidly transmitted through digital channels.

Table 4: Proximity to Bank Failures: Crisis Window Interactions

Panel A: GEO × Crisis Windows (2000–2023)		
Dependent Variables:	MES	$\Delta CoVaR$
Model:	(1)	(2)
Variables		
Geographic Proximity (t-1)	0.008	0.002
	(0.005)	(0.005)
Geographic Proximity (t-1) × GFC	0.05***	0.04**
	(0.02)	(0.01)
Geographic Proximity (t-1) × 2023	-0.04	-0.01
	(0.03)	(0.04)
Bank FE	Yes	Yes
Time FE	Yes	Yes
Bank Controls	Yes	Yes
Fit statistics		
Observations	27,598	27,598
R^2	0.66241	0.70875
Panel B: SCI × Crisis Windows (2013–2023)		
Dependent Variables:	MES	$\Delta CoVaR$
Model:	(1)	(2)
Variables		
Social Proximity (t-1)	-0.003	0.006
	(0.004)	(0.005)
Social Proximity (t-1) × 2023	0.28	0.39*
	(0.17)	(0.20)
Bank FE	Yes	Yes
Time FE	Yes	Yes
Bank Controls	Yes	Yes
Fit statistics		
Observations	10,374	10,374
R^2	0.79310	0.83775

Notes: Bank controls are included in all regressions but not reported.

4.4 Social Proximity, Sentiment, and Crisis

We further examine whether the effect of social proximity on systemic risk depends jointly on sentiment and the crisis regime. The specification extends the baseline by adding interactions between social proximity, local Twitter sentiment, and the 2023 crisis indicator:

$$\begin{aligned}\mathrm{SR}_{b,t} = {} & \mu_b + \lambda_t + \beta_1\,\text{Social Proximity}_{b,t-1} + \beta_2\,\text{Sentiment}_{b,t-1} + \beta_3\,(\text{Social Proximity} \times \text{Sentiment})_{b,t-1} \\ & + \beta_4\,\mathbf{1}_{2023} + \beta_5\,(\text{Social Proximity} \times \mathbf{1}_{2023})_{b,t-1} + \beta_6\,(\text{Sentiment} \times \mathbf{1}_{2023})_{b,t-1} \\ & + \beta_7\,(\text{Social Proximity} \times \text{Sentiment} \times \mathbf{1}_{2023})_{b,t-1} + \gamma'\,\mathbf{X}_{b,t-1} + \epsilon_{b,t}\end{aligned}$$

The coefficient of interest is β_7, which captures whether sentiment shapes the effect of social proximity on systemic risk differently during the 2023 crisis relative to normal times.

Table 5 reports the results. In normal times, social proximity alone does not significantly elevate systemic risk, consistent with social networks transmitting mixed signals in the absence of a common shock. Sentiment on its own is negative and significant for ΔCoVaR (-0.04^{**}), suggesting that positive sentiment reduces a bank's contribution to system-wide distress during non-crisis periods.

Table 5 also shows that the Sentiment×2023 interaction is significant for both MES (0.49^{***}) and ΔCoVaR ($0.36*$), indicating that positive sentiment reduces systemic risk during the crisis through the direct sentiment channel, independent of social proximity. This suggests that the sentiment exhibited on social media matters for system-wide distress regardless of how socially connected a bank's region is.

The triple interaction β_7 is negative and significant for MES (-2.2^{**}) but not for ΔCoVaR. Negative local sentiment strengthens the association between social proximity to failures and systemic risk, while positive sentiment attenuates it. The significant triple interaction for MES then shows that social proximity further intensifies this effect: sentiment's association with own-bank tail risk is stronger precisely in regions with greater social connectedness to failure counties, consistent with social networks amplifying the reach of the local information environment during stress.

The negative sign on β_7 implies that during the 2023 crisis, rising sentiment reduces systemic risk among socially connected banks, while falling sentiment amplifies it. The former is consistent with reassuring public communication, such as the FDIC's decision to guarantee all deposits, traveling through social networks and containing contagion. The latter aligns with Cookson et al. (2026) and Bales and Burghof (2024), who document how coordinated negative posts on Twitter accelerated deposit withdrawals and fueled SVB's collapse.

Table 5: Social Proximity, Sentiment, Crisis

Dependent Variables:	MES	$\Delta CoVaR$
Model:	(1)	(2)
Variables		
Social Proximity (t-1)	-0.006	0.002
	(0.005)	(0.005)
Average Twitter Sentiment (t-1)	-0.02	-0.04**
	(0.02)	(0.02)
Social Proximity (t-1) × Average Twitter Sentiment (t-1)	-0.004	-0.007
	(0.005)	(0.005)
Social Proximity (t-1) × 2023	0.03	0.23
	(0.17)	(0.22)
Average Twitter Sentiment (t-1) × 2023	-0.49***	-0.36*
	(0.17)	(0.20)
Social Proximity (t-1) × Average Twitter Sentiment (t-1) × 2023	-2.2**	-1.4
	(0.89)	(1.1)
Bank FE	Yes	Yes
Time FE	Yes	Yes
Bank Controls	Yes	Yes
Fit statistics		
Observations	10,374	10,374
R^2	0.79372	0.83829

Notes: Bank controls are included but not reported.

Figure 6 reports the implied marginal effects of social proximity on MES and ΔCoVaR at sentiment equal to −1, 0, and +1 standard deviations, separately for normal times and the 2023 crisis period. The standard errors are computed via the delta method. In normal times, the marginal effects are small and statistically indistinguishable from zero across all sentiment levels for both measures of systemic risk MES and ΔCoVaR. During the 2023 crisis, the marginal effect on MES varies monotonically with sentiment: strongly positive at low sentiment (2.178, SE = 0.851, t = 2.56), near zero at the median (0.020, SE = 0.172, t = 0.12), and negative at high sentiment (2.138, SE = 0.954, t = 2.24). Social proximity amplifies a bank's own tail risk when the surrounding information environment is pessimistic and attenuates it when sentiment is positive. For ΔCoVaR, the 2023 marginal effects follow the same directional pattern but do not reach conventional significance levels.

A notable divergence emerges across Tables 4 and 5. In Table 4, the Social Proximity ×2023 interaction is significant for ΔCoVaR (0.39*) but not MES, suggesting that during the 2023 episode, social connectedness to failure counties is associated with elevated systemic contribution before accounting for the local sentiment environment. In Table 5, once sentiment is fully interacted with social proximity and the crisis indicator, the triple interaction is significant for MES but not ΔCoVaR. These results suggest that social proximity operated through two distinct channels during 2023. The first is a structural channel: social connectedness elevated a bank's contribution to system-wide distress during 2023 regardless of the local sentiment environment. The second is an informational channel: social connectedness amplified a bank's own tail risk exposure specifically when the local sentiment environment was pessimistic, and attenuated it when sentiment was positive. The marginal effects in Figure 6 illustrate this pattern in detail.

The results are consistent with Wake-up Call dynamics: social network structure shapes how the broader depositor and investor community incorporates stress signals from nearby failures, rather than reflecting the initial institutional shock itself. Proximity determines which banks are first exposed to the signal that an institutional failure sends, and the local sentiment environment determines how forcefully that signal translates into systemic risk.[7]

[7]While some evidence suggests social media panic was a symptom of underlying balance sheet vulnerabilities rather than an independent cause (Kelly and Rose 2025), our results pertain to how network structure shapes risk transmission across the banking sector, regardless of the initiating mechanism.

Figure 6: Social Proximity, Sentiment, Crisis - Marginal Effects

Panel A: Marginal Effects Table

Regime	Sentiment (SD)	$\frac{\partial Y}{\partial \text{SCI}}$ (MES)	$\frac{\partial Y}{\partial \text{SCI}}$ (ΔCoVaR)
Normal	-1	-0.002 (0.004)	0.008 (0.005)
Normal	0	-0.006 (0.005)	0.002 (0.005)
Normal	1	-0.010 (0.010)	-0.005 (0.008)
2023	-1	2.178 (0.851)	1.619 (1.017)
2023	0	0.020 (0.172)	0.228 (0.218)
2023	1	-2.138 (0.954)	-1.164 (1.129)

Notes: Entries report the implied marginal effect of social proximity on the outcome at sentiment equal to -1, 0, and +1 standard deviations, by regime. Standard errors are computed via the delta method using the estimated variance-covariance matrix.

Panel B: Marginal Effects Plot

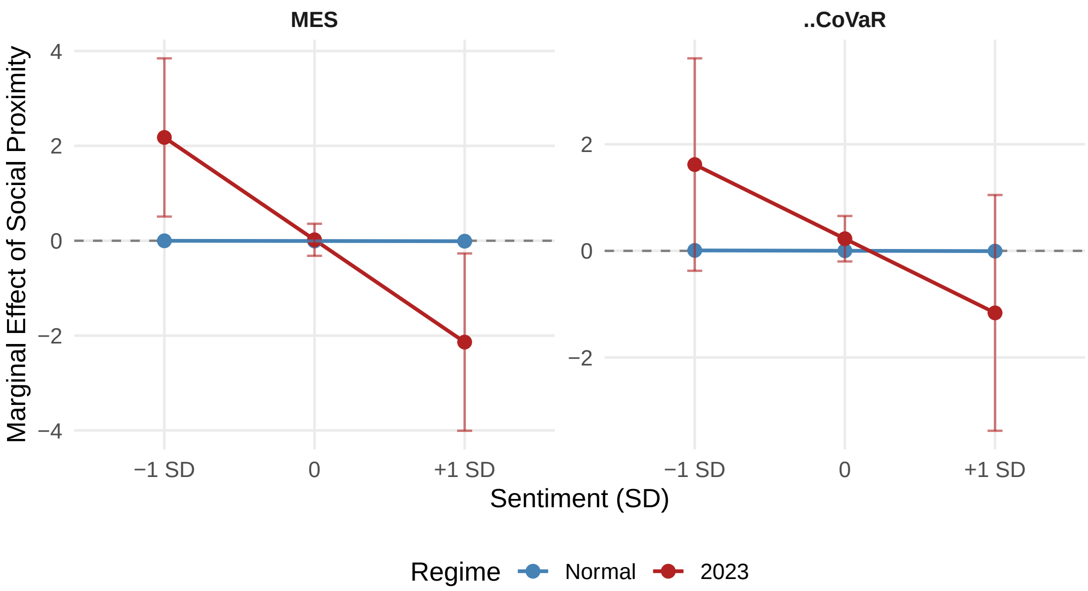

Notes: Marginal effects of social proximity on MES and ΔCoVaR at sentiment equal to -1, 0, and $+1$ standard deviations, by regime. Whiskers show 95% confidence intervals computed via the delta method.

4.5 Robustness Checks

A potential concern with the baseline specifications is that the proximity measures may capture region-specific shocks rather than network-based transmission. We assess whether the baseline findings survive more stringent controls for regional confounding. For instance, banks geographically close to failures may simply be exposed to the same local economic conditions, rather than experiencing contagion through proximity per se. To address this, we replace year-quarter fixed effects with region$\times$year-quarter fixed effects, absorbing any time-varying shocks common to banks within the same region. The way each bank is classified into each region is shown in

Table A5.

Tables A4 and A3 report the results. The geographic proximity coefficient remains positive and significant for both MES (0.0227^{**}) and ΔCoVaR (0.0175^{**}), and the social proximity results retain their sign and remain statistically insignificant — consistent with the baseline findings. Therefore the baseline findings are unlikely to be driven by regional economic conditions that happen to correlate with bank failure clusters.

We do not include more granular branch-level geographic fixed effects. Each bank holding company operates branches across multiple counties and regions, a single location-based fixed effect cannot adequately characterize a bank's geographic exposure. The deposit-weighted proximity measures already account for this by aggregating each bank's exposure across its full branch network. Imposing fixed effects based on headquarters location alone would introduce a mismatch between the variation the fixed effect absorbs and the variation the proximity measure captures, which could understate the geographic channel. The region$\times$year-quarter fixed effects offer a conservative alternative that addresses the regional confounding concern without this complication.

5 Conclusion

Our findings show that the transmission of systemic risk extends beyond direct balance-sheet linkages. Geographic proximity to bank failures is consistently associated with elevated systemic risk over the full sample period, while social proximity becomes a particularly important channel during the 2023 banking stress episode, conditional on the local sentiment environment. Together, these results highlight two dimensions of contagion, spatial and social, that are not typically incorporated into standard surveillance of financial fragility.

Although our analysis does not isolate the precise mechanisms through which proximity translates into tail risk, it provides new empirical evidence that network structure is an economically meaningful correlate of contagion dynamics. An important next step is to sharpen identification using plausibly exogenous variation in connectedness, such as interstate branching deregulation for geographic exposure or historically determined migration patterns for social connectedness.

At the same time, the 2023 episode underscores the practical relevance of these patterns. The same social channels through which panic can spread may also transmit stabilizing information. In that sense, timely public communication (such as the FDIC's decision to guarantee all deposit) may be especially effective when it reaches highly connected communities quickly and credibly. Measures such as the Social Connectedness Index may therefore help regulators identify counties where stress signals are most likely to amplify and where targeted communication could complement broader crisis interventions.

A Appendix

Table A1: Geographic Proximity Baseline with all Controls 2000-2023

Dependent Variables:	MES	$\Delta CoVaR$
Model:	(1)	(2)
Variables		
Geographic Proximity (t-1)	0.03^{***}	0.02^{**}
	(0.008)	(0.007)
Log Assets (t-1)	0.44^{***}	0.10
	(0.07)	(0.07)
Unrealized HTM Losses Book Ratio (t-1)	0.009	0.009
	(0.01)	(0.01)
Cash Asset Ratio (t-1)	0.02^{*}	0.03^{**}
	(0.01)	(0.01)
Liquid Asset Ratio (t-1)	-0.006	0.01
	(0.02)	(0.02)
Loans Asset Ratio (t-1)	0.08^{***}	0.06^{**}
	(0.03)	(0.03)
Leverage (t-1)	-0.02	0.13^{**}
	(0.07)	(0.05)
Deposits Liabilities Ratio (t-1)	-0.05^{*}	-0.04
	(0.03)	(0.02)
Non-Interest Income Ratio (t-1)	0.02	-0.01
	(0.02)	(0.02)
Bank FE	Yes	Yes
Time FE	Yes	Yes
Fit statistics		
Observations	27,598	27,598
R^2	0.66175	0.70845

Notes: All bank control coefficients are reported.

Table A2: Social Proximity Baseline with all Controls 2013-2023

Dependent Variables:	MES	$\Delta CoVaR$
Model:	(1)	(2)
Variables		
Social Proximity (t-1)	-0.003	0.007
	(0.004)	(0.004)
Log Assets (t-1)	0.49**	0.06
	(0.20)	(0.14)
Unrealized HTM Losses Book Ratio (t-1)	-0.02	-0.009
	(0.02)	(0.01)
Cash Asset Ratio (t-1)	0.010	0.01
	(0.02)	(0.02)
Liquid Asset Ratio (t-1)	0.02	0.11***
	(0.04)	(0.04)
Loans Asset Ratio (t-1)	0.13**	0.14**
	(0.06)	(0.06)
Leverage (t-1)	0.03**	0.04*
	(0.01)	(0.02)
Deposits Liabilities Ratio (t-1)	-0.03	-0.03
	(0.06)	(0.06)
Non-Interest Income Ratio (t-1)	0.006	-0.03
	(0.03)	(0.03)
Bank FE	Yes	Yes
Time FE	Yes	Yes
Fit statistics		
Observations	10,374	10,374
R^2	0.79290	0.83737

Notes: All bank control coefficients are reported.

Table A3: Robustness: Social Proximity and Twitter Sentiment with Region × Year-Quarter Fixed Effects

Dependent Variables:	MES	$\Delta CoVaR$	MES	$\Delta CoVaR$
Model:	(1)	(2)	(3)	(4)
Variables				
Social Proximity (t-1)	-0.0024	0.0047	-0.0046	0.0016
	(0.0038)	(0.0048)	(0.0053)	(0.0046)
Log Assets (t-1)	0.4476**	0.0225	0.4468**	0.0213
	(0.1873)	(0.1267)	(0.1875)	(0.1268)
Unrealized HTM Losses Book Ratio (t-1)	-0.0189	-0.0118	-0.0186	-0.0112
	(0.0165)	(0.0100)	(0.0164)	(0.0099)
Cash Asset Ratio (t-1)	0.0170	0.0208	0.0178	0.0219
	(0.0227)	(0.0196)	(0.0227)	(0.0196)
Liquid Asset Ratio (t-1)	0.0069	0.0952***	0.0074	0.0959***
	(0.0330)	(0.0336)	(0.0333)	(0.0339)
Loans Asset Ratio (t-1)	0.1321**	0.1346***	0.1354**	0.1396***
	(0.0551)	(0.0517)	(0.0554)	(0.0517)
Leverage (t-1)	0.0291**	0.0369*	0.0286**	0.0362*
	(0.0133)	(0.0214)	(0.0131)	(0.0209)
Deposits Liabilities Ratio (t-1)	-0.0245	-0.0386	-0.0262	-0.0411
	(0.0553)	(0.0499)	(0.0555)	(0.0505)
Non-Interest Income Ratio (t-1)	0.0177	-0.0190	0.0174	-0.0194
	(0.0244)	(0.0246)	(0.0244)	(0.0245)
Average Twitter Sentiment (t-1)			-0.0271	-0.0407**
			(0.0179)	(0.0173)
Social Proximity (t-1) × Average Twitter Sentiment (t-1)			-0.0040	-0.0056
			(0.0054)	(0.0050)
Fixed-effects				
Region × Time FE	Yes	Yes	Yes	Yes
Bank FE	Yes	Yes	Yes	Yes
Fit statistics				
Observations	10,374	10,374	10,374	10,374
R^2	0.79836	0.84242	0.79846	0.84264
Within R^2	0.02020	0.01094	0.02068	0.01232

Clustered (Bank FE) standard-errors in parentheses
*Signif. Codes: ***: 0.01, **: 0.05, *: 0.1*

Region×year-quarter fixed effects absorb region-specific shocks at each quarter. Bank controls are included but not reported.

Table A4: Robustness: Geographic Proximity with Region × Year-Quarter Fixed Effects

Dependent Variables:	MES	$\Delta CoVaR$
Model:	(1)	(2)
Variables		
Geographic Proximity (t-1)	0.0227**	0.0175**
	(0.0092)	(0.0080)
Log Assets (t-1)	0.4625***	0.1201*
	(0.0738)	(0.0710)
Unrealized HTM Losses Book Ratio (t-1)	0.0073	0.0086
	(0.0113)	(0.0110)
Cash Asset Ratio (t-1)	0.0269*	0.0320**
	(0.0138)	(0.0136)
Liquid Asset Ratio (t-1)	-0.0103	0.0103
	(0.0209)	(0.0190)
Loans Asset Ratio (t-1)	0.0887***	0.0727**
	(0.0326)	(0.0300)
Leverage (t-1)	-0.0045	0.1425***
	(0.0634)	(0.0478)
Deposits Liabilities Ratio (t-1)	-0.0413	-0.0358
	(0.0299)	(0.0258)
Non-Interest Income Ratio (t-1)	0.0175	-0.0156
	(0.0176)	(0.0230)
Fixed-effects		
Region × Time FE	Yes	Yes
Bank FE	Yes	Yes
Fit statistics		
Observations	27,227	27,227
R^2	0.66960	0.71355
Within R^2	0.02419	0.00751

Clustered (Bank FE) standard-errors in parentheses
*Signif. Codes: ***: 0.01, **: 0.05, *: 0.1*

Region×year-quarter fixed effects absorb region-specific shocks at each quarter. Bank controls are included but not reported.

Table A5: Regional Classification of U.S. States

Region	States
Northeast	CT, ME, MA, NH, RI, VT, NJ, NY, PA
Midwest	IL, IN, MI, OH, WI, IA, KS, MN, MO, NE, ND, SD
South	DE, FL, GA, MD, NC, SC, VA, DC, WV, AL, KY, MS, TN, AR, LA, OK, TX
West	AZ, CO, ID, MT, NV, NM, UT, WY, AK, CA, HI, OR, WA

Notes: Regional classifications follow the U.S. Census Bureau definitions. States are assigned to regions based on county FIPS codes where available, with ZIP code as a fallback.

Table A6: Bank Holding Company Y9-C Data

Variable	**FR Y-9C Series Code**
cash and securities	BHCK0081 + BHCK0395 + BHCK0397 + BHCKJJ34 + BHCK1773 + BHCKJA22
cash	BHCK0081 + BHCK0395 + BHCK0397
securities	BHCKJJ34 + BHCK1773 + BHCKJA22
liabilities	BHCK2948
total_loans	BHCK5369 + BHCKB528
hold to maturity securities	BHCKJJ34
unrealized_htm_losses	BHCK1754 - BHCK1771
htm_book	BHCK1754
assets	BHCK2170
equity	BHCK2170 - BHCK2948
noninterest_income	BHCK4079
interest_income	BHCK4107

Note: Date range is 2000:I to 2023:IV.

Table A7: Bank Ratios

Variable	**Formula**
`log_assets`	ln(assets)
`leverage`	liabilities/equity
`unrealized_htm_losses_rat_book`	unrealized_htm_losses/htm_book
`liquid_asset_ratio`	cash_securities/assets
`cash_asset_ratio`	cash/assets
`securities_asset_ratio`	securities/assets
`loans_asset_ratio`	total_loans/assets
`deposits_liabilities_ratio`	deposits/liabilities
`noninterest_inc_ratio`	noninterest income/(noninterest income+ interest income)

Table A8: Data Sources for Variables used in Systemic Risk Calculations

Variable	Definition / Construction	Source
FFR	Federal Funds Rate	FRED
TBILL_DELTA	Percent change in the 3M Treasury Bill rate	FRED
CREDIT_SPREAD	BAA Corporate Bond rate minus 10Y Treasury Bond rate	FRED
LIQUIDITY_SPREAD	3M GC Repo rate minus 3M Treasury Bill rate	FRED
TED_SPREAD	3M USD LIBOR minus 3M Treasury Bill rate	FRED
YIELD_SPREAD	10Y Treasury Bond rate minus 3M Treasury Bond rate	FRED
DJ_CA_EXC	Excess returns of the DJ US Composite Average over S&P 500	Compustat
DJ_RESI_EXC	Excess returns of the DJ US Select Real Estate Securities Index over S&P 500	Compustat
VIX	Implied volatility index (equity market volatility)	CBOE / Compustat
S&P 500 Index	Broad equity market index	CRSP

References

Acemoglu, D., Ozdaglar, A., & Tahbaz-Salehi, A. (2015). Systemic risk and stability in financial networks. *American Economic Review*, *105*(2), 564–608.

Acharya, V. V., Pedersen, L. H., Philippon, T., & Richardson, M. (2017). Measuring systemic risk. *The Review of Financial Studies*, *30*(1), 2–47. https://doi.org/10.1093/rfs/hhw006

Adasi Manu, S., & Qi, Y. (2023). Ceo social connections and bank systemic risk: The "dark side" of social networks. *Journal of Banking and Finance*, *156*, 106988. https://doi.org/https://doi.org/10.1016/j.jbankfin.2023.106988

Adrian, T., & Brunnermeier, M. K. (2016). Covar. *American Economic Review*, *106*(7), 1705–41. https://doi.org/10.1257/aer.20120555

Ahnert, T., & Bertsch, C. (2022). A wake-up call theory of contagion. *Review of Finance*, *26*(4), 829–854.

Allen, F., & Gale, D. (2000). Financial contagion. *Journal of Political Economy*, *108*(1), 1–33.

Babus, A. (2016). The formation of financial networks. *RAND Journal of Economics*, *47*(2), 239–272.

Bailey, M., Cao, R., Kuchler, T., Stroebel, J., & Wong, A. (2018). Social connectedness: Measurement, determinants, and effects. *Journal of Economic Perspectives*, *32*(3), 259–280.

Bailey, M., Johnston, D., Kuchler, T., Stroebel, J., & Wong, A. (2020). Social connectedness in urban areas. *Journal of Urban Economics*, *118*, 103264.

Baker, M., & Wurgler, J. (2006). Investor sentiment and the cross-section of stock returns. *The journal of Finance*, *61*(4), 1645–1680.

Bales, S., & Burghof, H.-P. (2024). Public attention, sentiment and the default of silicon valley bank. *The North American Journal of Economics and Finance*, *69*, 102026. https://doi.org/10.1016/j.najef.2023.102026

Belluzzo, T. (2024). Systemic risk [https://github.com/TommasoBelluzzo/SystemicRisk/releases/tag/v3.6.0, GitHub, retrieved April 10, 2024].

Bikhchandani, S., Hirshleifer, D., & Welch, I. (1992). A theory of fads, fashion, custom, and cultural change as informational cascades. *Journal of Political Economy*, *100*(5), 992–1026.

Bikhchandani, S., Hirshleifer, D., & Welch, I. (1998). Learning from the behavior of others: Conformity, fads, and informational cascades. *Journal of Economic Perspectives*, *12*(3), 151–170.

Blume, L., Easley, D., Kleinberg, J., Kleinberg, R., & Tardos, É. (2011). Which networks are least susceptible to cascading failures? *Proceedings of the 2011 52nd IEEE Annual Symposium on Foundations of Computer Science*, 393–402.

Blume, L., Easley, D., Kleinberg, J., Kleinberg, R., & Tardos, É. (2013). Network formation in the presence of contagious risk. *ACM Transactions on Economics and Computation*, *1*(2).

Bostandzic, D., & Weiss, G. N. F. (2018). Why do some banks contribute more to systemic risk than others? *Journal of Financial Intermediation*, *35*, 17–40.

Brunnermeier, M. K., Dong, G. N., & Palia, D. (2020). Banks' noninterest income and systemic risk. *The Review of Corporate Finance Studies*, *9*(2), 229–255.

Cabrales, A., Gottardi, P., & Vega-Redondo, F. (2017). Risk sharing and contagion in networks. *The Review of Financial Studies*, *30*(9), 3086–3127. https://doi.org/10.1093/rfs/hhx077

Calomiris, C. W., & Mason, J. R. (1994, November). *Contagion and bank failures during the great depression: The june 1932 chicago banking panic* (NBER Working Paper No. 4934). National Bureau of Economic Research. https://doi.org/10.3386/w4934

Chai, Y., Kakkar, D., Palacios, J., et al. (2023). Twitter sentiment geographical index dataset. *Scientific Data*, *10*, 684. https://doi.org/10.1038/s41597-023-02572-7

Chan-Lau, J., Espinosa-Vega, M., Giesecke, K., & Sole, J. (2009). Assessing the systemic implications of financial linkages. In *Imf global financial stability report* (Vol. 2).

Choi, D. B., Goldsmith-Pinkham, P., & Yorulmazer, T. (2023). *Contagion effects of the silicon valley bank run* (tech. rep. No. w31772). National Bureau of Economic Research.

Clements, A., Hurn, S., & Shi, S. (2017). An empirical investigation of herding in the u.s. stock market. *Economic Modelling*, *67*, 184–192. https://doi.org/10.1016/j.econmod.2016.12.015

Cookson, J. A., Fox, C., Gil-Bazo, J., Imbet, J. F., & Schiller, C. (2026). Social media as a bank run catalyst. *Journal of Financial Economics*, *176*, 104218.

Cornett, M. M., McNutt, J. J., Strahan, P. E., & Tehranian, H. (2011). Liquidity risk management and credit supply in the financial crisis. *Journal of Financial Economics*, *101*(2), 297–312.

De Long, J. B., Shleifer, A., Summers, L. H., & Waldmann, R. J. (1990). Noise trader risk in financial markets. *Journal of political Economy*, *98*(4), 703–738.

Diamond, D. W., & Dybvig, P. H. (1983). Bank runs, deposit insurance, and liquidity. *Journal of Political Economy*, *91*(3), 401–419.

Duan, Y., El Ghoul, S., Guedhami, O., Li, H., & Li, X. (2021). Bank systemic risk around covid-19: A cross-country analysis. *Journal of Banking & Finance*, *133*, 106299.

Ellis, S., Sharma, S., & Brzeszczyński, J. (2022). Systemic risk measures and regulatory challenges. *Journal of Financial Stability*, *61*, 100960.

Fang, Y., Wang, Q., Wang, Y., & Yuan, Y. (2024). Media sentiment, deposit stability and bank systemic risk: Evidence from china. *International Review of Economics & Finance*, *91*, 1150–1172. https://doi.org/10.1016/j.iref.2024.01.067

Flynn, S., & Wang, J. (2022). Social connections and bank deposit funding. *Available at SSRN 4058650*.

Freixas, X., Parigi, B. M., & Rochet, J.-C. (2000). Systemic risk, interbank relations, and liquidity provision by the central bank. *Journal of Money, Credit and Banking*, 611–638.

Goldstein, M. (1998). *Contagion: A review of the literature*. Institute for International Economics.

Hirshleifer, D., Peng, L., & Wang, Q. (2025). News diffusion in social networks and stock market reactions. *The Review of Financial Studies*, *38*(3), 883–937.

Holmes, P., Kallinterakis, V., & Leite Ferreira, M. (2013). Herding in a concentrated market: A question of intent. *European Financial Management*, *19*(3), 497–520.

Hong, H., Kubik, J. D., & Stein, J. C. (2004). Social interaction and stock-market participation. *The journal of finance*, *59*(1), 137–163.

Hong, H., & Stein, J. C. (1999). A unified theory of underreaction, momentum trading, and overreaction in asset markets. *The Journal of Finance*, *54*(6), 2143–2184.

Kelly, M., & Ó Gráda, C. (2000). Market contagion: Evidence from the panics of 1854 and 1857. *American Economic Review*, *90*(5), 1110–1124.

Kelly, S., & Rose, J. D. (2025). *Rushing to judgment and the banking crisis of 2023* (tech. rep.). Federal Reserve Bank of Chicago Working Paper No. 2025-04.

Krause, A., & Giansante, S. (2012). Interbank lending and the spread of bank failures: A network model of systemic risk. *Journal of Economic Behavior & Organization*, *83*(3), 583–608.

Laeven, L., Ratnovski, L., & Tong, H. (2016). Bank size, capital, and systemic risk. *Journal of Banking & Finance*, *69*, S25–S34.

Löffler, G., & Raupach, P. (2018). Pitfalls in the use of systemic risk measures. *Journal of Financial and Quantitative Analysis*, *53*(1), 269–298.

Mizruchi, M. S., & Stearns, L. B. (2001). Getting deals done: The use of social networks in bank decision-making. *American sociological review*, *66*(5), 647–671.

Sedunov, J. (2016). What is the systemic risk exposure of financial institutions? *Journal of Financial Stability*, *24*, 71–87.

Shiller, R. J. (2000). *Irrational exuberance*. Princeton University Press.

Shiller, R. J. (2017). Narrative economics. *American Economic Review*, *107*(4), 967–1004. https://doi.org/10.1257/aer.107.4.967

Wheelock, D. C. (1992). Regulation and bank failures: New evidence from the agricultural collapse of the 1920s. *The Journal of Economic History*, *52*(4), 806–825.

Wu, Y., Lee, C.-C., Lee, C.-C., & Peng, D. (2022). Geographic proximity and corporate investment efficiency: Evidence from high-speed rail construction in china. *Journal of Banking and Finance*, *140*, 106510. https://doi.org/https://doi.org/10.1016/j.jbankfin.2022.106510